INTERNATIONAL JOURNAL OF ADAPTIVE CONTROL AND SIGNAL PROCESSING
Int. J. Adapt. Control Signal Process. 2001; **15**:697–713 (DOI:10.1002/acs.629)

A unified adaptive oculomotor control model*

Xiaolin Zhang† and Hidetoshi Wakamatsu

School of Medicine, Tokyo Medical and Dental University, 1-5-45 Yushima, Bunkyo-ku, Tokyo 113, Japan

SUMMARY

In order to understand mechanisms of oculomotor control systems, an oculomotor model based on eye's anatomical structure and physiological mechanism is developed. In this model, various types of eye movements are considered, and two learning systems, one based on adaptive characteristics of flocculus and the other on vestibular nuclei's are developed. The role of neural paths from ocular muscle stretch receptors into flocculus, which were thought to not contribute in eye movement, is discussed in detail from the viewpoint of system control engineering. The experimental results through simulation show good control performance of the proposed model. Copyright © 2001 John Wiley & Sons, Ltd.

KEY WORDS: eye movement system; flocculus; vestibular nuclei; learning system; neural network

1. INTRODUCTION

When catching a moving object on the *central pit* of the retina, the oculomotor control system performs different kinds of eye movements according to position and movements of target and head. To understand the anatomic structure and the physiological mechanism of eye, a mathematical model for the oculomotor control system is needed.

Until now, most eye movement models simulated only one type of movement [1–3]. However, most eye movements are composed of several types, which co-ordinate with each other. Further, some eye movements, such as smooth pursuit and optokinetic reflex, though with different input signals from the retina, are controlled by the same neural loop, and are always generated together and cannot be divided from the viewpoint of physiological mechanism. Thus, in order to analyse characteristics of unified eye movements, a model including control loops of smooth pursuit, optokinetic reflex, and VOR (vestibuloocular reflex) are built.

It is known that eye shows adaptability to variation of environment and physiological changes [2–14]. Recently, it has become clear that this adaptability is shown not only in the flocculus but

*This study was partly presented in European Control Conference in 1999.
†Correspondence to: Xiaolin Zhang, School of Medicine, Tokyo Medical and Dental University, 1-5-45 Yushima, Bunkyo-ku, Tokyo 113, Japan.

Contract/grant sponsor: Ministry of Education of Japan
Contract/grant sponsor: Mitsubishi Foundation

Received 19 April 1999
Published online 22 March 2001 *Revised 6 February 2000*
Accepted 18 June 2000

also in the brain stem [5–9]. However, how the two adaptive systems, referred below as learning systems, are related to each other, and the merits of the two learning systems working together had not been discussed. This paper analyses the characteristics and relationships of the two learning systems using learning models from the viewpoint of system control engineering.

2. OCULOMOTOR CONTROL SYSTEM MODEL

Eye movements are classified in saccade, smooth pursuit, optokinetic reflex, VOR, and vergence. In order to make the discussion easy, only horizontal movement for a single eye here is considered. Thus, vergence is not considered. Here saccade also is not considered, which has an independent eye movement control system, however, saccadic signal is taken into account as a reset signal when the optic axis angle is larger than the limited angle of eyeball.

2.1. Neuron paths of oculomotor system

Oculomotor neural paths are given by Figure 1 based on the previous studies [1–3, 11–15]. Figure 1 is regarded as a control system, eyeball and ocular muscles are the controlled objects, and angle E of the horizontal optic axis is the output of the system. The control loop of the head horizontal rotational signal detected by the horizontal canal (HC) is via vestibular nucleus (VN) → oculomotor nucleus (OMN) → medial rectus muscles (MR) or VN → abducent nucleus (AN) → lateral rectus muscles (LR). The control loop of the retina signal is from retina (R) → pretectum (PT) → nucleus reticularis tegmenti pontis (NRTP) → VN → OMN → MR or VN → AN → LR. Saccadic signals come from colliculus superior and input to VN.

The structure of flocculus will be described in Section 5. Here only the input and output signals of flocculus related to horizontal eye movements are introduced. The input signals are transferred through mossy fibers (mf). The signals coming from HC are head horizontal rotational signals, and the ones coming from NRTP are retinal slip signals and retinal slip velocity signals. The mfs from stretch receptors of eye muscles (LR, MR) are considered as paths to transfer the signals of

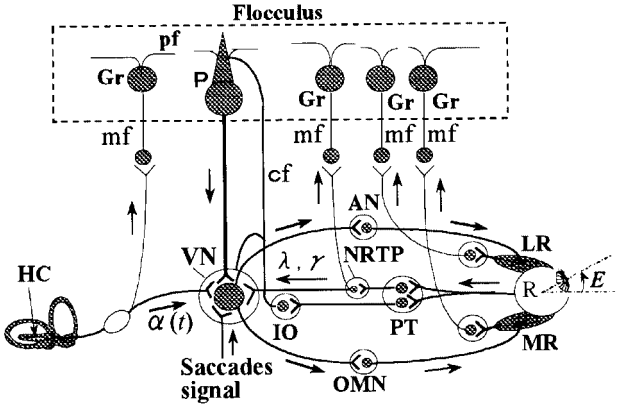

Figure 1. Outline of neural paths for eye movements.

eye rotational angle. The output of flocculus come from Purkinje's Cells (P) through axons, and input to VN.

The above control loops constitute a basic control system of eye movement, with flocculus as the learning system [4–16]. The learning error, which is used to improve the parameters of a learning system (referred below as teaching signal), is the retinal slip signal, which comes from the retina through IO (inferior olive nucleus) and cf (climbing fibers).

As climbing fibres, which transfer of the teaching signals, have branches connected to VN, the learning system of the brain stem is thought to be in the VN [12, 16]. Here, the synaptic transmission from HC to VN is expressed as $\alpha(t)$. The synaptic transmissions from NRTP to VN are expressed as λ and γ, where λ is gain of retinal slip signal transmission paths and γ is gain of retinal slip velocity signal transmission paths. Since control efficiency is not so sensitive to gains of feedback as to the ones of feedforward, synaptic transmissions of visual feedback loops (λ, γ) are regarded as constant. Therefore, the VN's learning system is expressed as a variable gain $\alpha(t)$ of feedforward path changed by climbing fibres.

2.2. *Mathematical model of oculomotor system*

The block diagram of eye movement control system based on Section 2.1 is illustrated in Figure 2. Considering only rotational movement of head and target, H_p is head rotational angle, O_t is target rotational angle around the neck, O_r is target rotational angle related to the head, H_v is signal from the semi-circular canals [1–3], O_v is retinal slip velocity, ε is retinal slip, and τ is delay for retinal slip detection. Optical axis angle $E(t)$ always moves in the opposite direction of head rotation, while the target is standstill. Therefore, $H(t) = -H_p(t)$ is used as input signal of the model. The flocculus is considered as a learning system, and we use an artificial neural network (ANN) to simulate it.

To simplify the discussion, the transfer function of the controlled object, namely, the total transfer function of the medial rectus muscles, the lateral rectus muscles, and the eyeball is considered as a first-order system, where T_e is time constant of the controlled object, g is gain. There is a neural integrator between the vestibular nucleus and the ocular motor nucleus or the abducent nucleus, so the transfer function of the neural paths from VN to LR and MR is

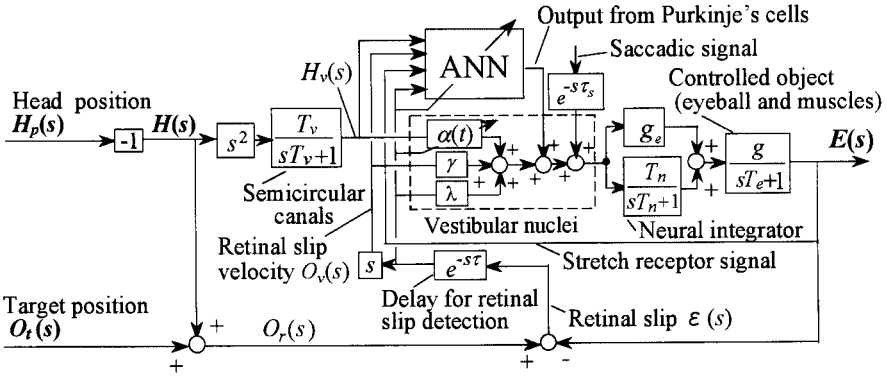

Figure 2. Eye movement control system for a single eye.

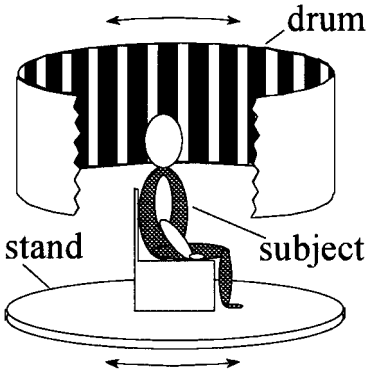

Figure 3. Concept of experiment.

expressed as the sum of an imperfect integrator[‡] and a direct path, where T_n is time constant of the integrator, and g_e is gain of the direct path [1]. The symbols $\alpha(t)$, γ and λ represent synaptic transmission gains of neural fibres that transfer head velocity signal, retinal slip velocity signal, and retinal slip signal. To simulate the learning mechanism of VN, $\alpha(t)$ is utilized by its learning capability.

3. DYNAMIC CHARACTERISTICS OF THE MODEL

In order to validate the characteristics of the model with those of the physiological mechanism, an experiment as illustrated in Figure 3 was performed using our proposed eye movement model, and the simulation results were compared with the experimental ones of past research [1, 17, 18]. Figure 3 shows a subject sitting on the centre of a stand inside a drum. The drum and/or the stand are rotated. In a short period of time, transmissions of paths through flocculus, which are changed by the learning system, can be considered as constant. Similarly, $\alpha(t)$ can be thought as a constant gain. In normal state [1], $T_n \gg g_e$. So, the following equation is obtained:

$$\frac{T_n}{sT_n + 1} + g_e = \frac{T_n(sg_e + 1)}{sT_n + 1} \quad (T_n \gg g_e) \tag{1}$$

When $g_e = T_e$, the pole of the controlled object $(sT_e + 1)$ will be cancelled. This pole-zero cancellation in eye movement control system has been confirmed by physiological experiments [1]. Here the gain of the controlled object is defined as $g = 1$. Thus, Figure 2 is simplified as shown by Figure 4, where α, γ and λ are constant gains, considering transmissions of paths through flocculus. $\alpha = 1$, $\gamma = 0.5$, $\lambda = 0.01$ are given based on physiological data [1, 11]. In

[‡]Physiological experiments have shown that the neural integrator has a loss. This means that the neural integrator can be expressed by $T_n/(sT_n + 1)$. When $T_n \to \infty$ the imperfect integrator becomes a perfect integrator $1/s$.

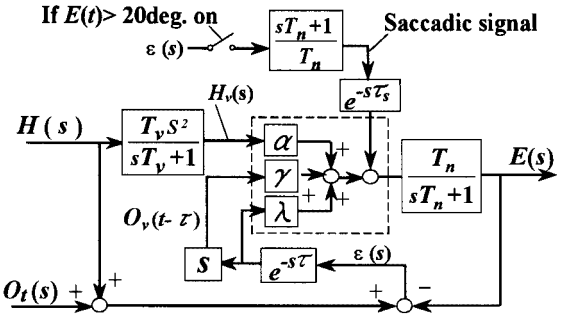

Figure 4. A simplified oculomotor control system without cerebellum.

Figure 4, the saccadic signal is produced by the retinal slip signal through inverse system of the neural integrator for $E(t)$ bigger than 20°. The following equation is obtained from Figure 4:

$$E(s) = \frac{T_n}{(T_n s + 1)}\left[\alpha \frac{T_v s^2}{T_v s + 1} H(s) + (\gamma s + \lambda) e^{-s\tau} \varepsilon(s)\right] \tag{2}$$

3.1. *Unification of main types of eye movements*

A unified eye movement of VOR, optokinetic reflex and smooth pursuit is produced by rotating the stand under the condition that the subject can watch the stripes on the drum. Through simulation, the stand rotated at 50 deg/s for 20 s, and stopped (the accelerations were 500 deg/s^2 in the first 0.1 s and -500 deg/s^2 in the last 0.1 s). The drum was fixed. Thus, in Figure 4

$$O_t(s) = 0, \quad \varepsilon(s) = H(s) - E(s) \tag{3}$$

Hence Equation (2) becomes

$$E(s) = \frac{\alpha T_v T_n s^2 + T_n(\gamma s + \lambda)(T_v s + 1) e^{-s\tau}}{(T_v s + 1)[(1 + \gamma e^{-s\tau}) T_n s + \lambda T_n e^{-s\tau} + 1]} H(s) \tag{4}$$

In normal state, utilizing the parameters as [1] $T_v = 15$ s, $T_n = 16$ s, $\tau = 0.12$ s, $\tau_s = 0.2$ s, the trajectory of the optical axis can be simulated using Equation (4). Figure 5 shows the simulation results. In Fig. 5(a) the smooth curve is smooth pursuit, and the abrupt curve is saccade. Figure 5(b) shows the velocity of the eyeball. The broken line is the head rotational velocity signal $H_v(t)$, which comes from the semicircular canals. The figure shows that the pursuit velocity is almost equal to the head rotational velocity $\dot{H}(t)$, which means that the unified model has as good a control performance as the normal physiological eye movement.

3.2. *VOR eye movement*

For the experiment in darkness, VOR is produced by rotating the stand. In this case, the eye movement control system cannot get the retinal slip signal, and eye movement is controlled only by the head movement signal that comes from the semicircular canals. The following equation is

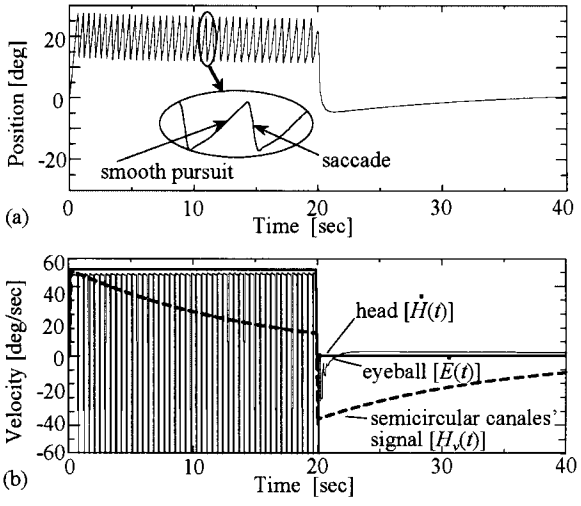

Figure 5. Characteristics of the model in normal state.

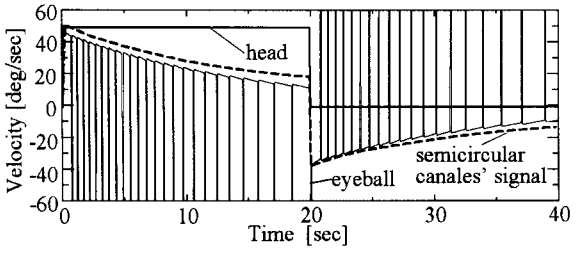

Figure 6. Characteristics of the model for VOR.

obtained from Equation (2):

$$E(s) = \frac{\alpha T_n T_v s^2}{(T_n s + 1)(T_v s + 1)} H(s) \tag{5}$$

The stand was set to rotate at 50 deg/s. The output of the semi-circular canals is the head velocity, which has a loss, and the neural integrators between the vestibular nucleus and the oculomotor nucleus or the abducent nucleus also have a loss [1]. Thus, if head rotates at a constant velocity, the eyeball velocity is near the head velocity at the first instant, and becomes zero slowly. Figure 6 shows trajectory of the optic axis calculated from Equation (5). This phenomenon appears in physiological experiments [1].

3.3. Optokinetic eye movement

If the drum is rotated and the head is fixed, Equation (2) becomes

$$E(s) = \frac{T_n(\gamma s + \lambda)e^{-s\tau}}{(T_n s + 1) + T_n(\gamma s + \lambda)e^{-s\tau}} O_t(s) \tag{6}$$

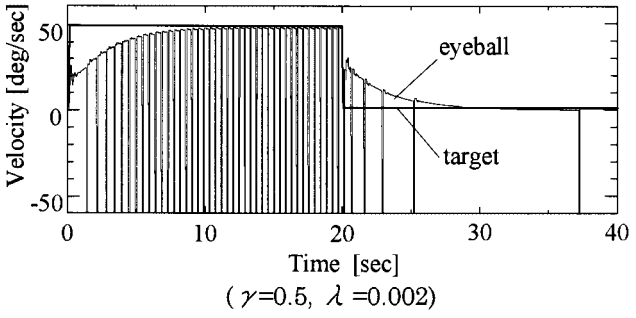

Figure 7. Characteristics of optokinetic eye movement.

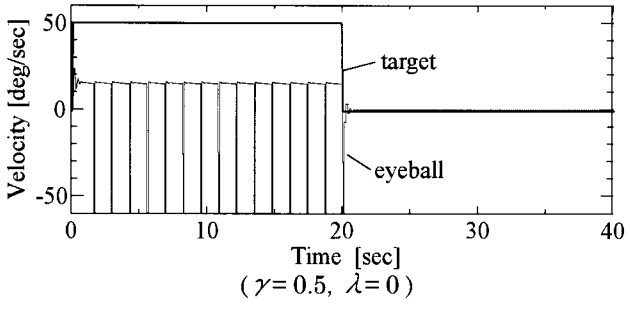

Figure 8. If set $\lambda = 0$ the optokinetic eye movement has only the fast component.

The output $E(s)$ of the model is expressed in Figure 7 using Equation (6). Figure 7 shows that the velocity of optokinetic nystagmus has 2 parts, a fast component and a slow component. Here the feedback gain λ is reset to a smaller value 0.002 in order to obtain a clear curve of the slow component. This phenomenon appears in physiological experiments [17].

If the signal of the retinal slip is cut by setting $\lambda = 0$, the output of the model has only the fast component (Figure 8), and if the signal of the retinal slip velocity is cut by setting $\gamma = 0$, the output of the model is given as only the slow component (Figure 9) [11].

It is demonstrated through simulation, that the fast component of optokinetic nystagmus is caused by the retinal slip velocity signal, and that the slow component is caused by the retinal slip signal.

3.4. Side effects of VOR

If the drum rotates at the same velocity as the stand, signals from the semi-circular canals prevent the eye from gazing the target (a stripe drawn on the drum). In this case the eyeball need not move, though signals are sent from the semicircular canals to the vestibular nucleus. Since

$$H(s) = -O_t(s), \quad \varepsilon(s) = -E(s) \tag{7}$$

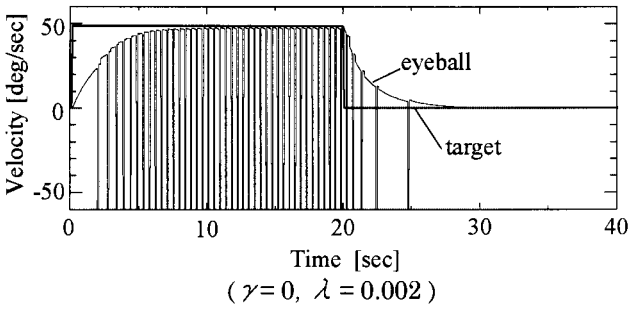

Figure 9. If set $\gamma = 0$ the optokinetic eye movement has only the slow component.

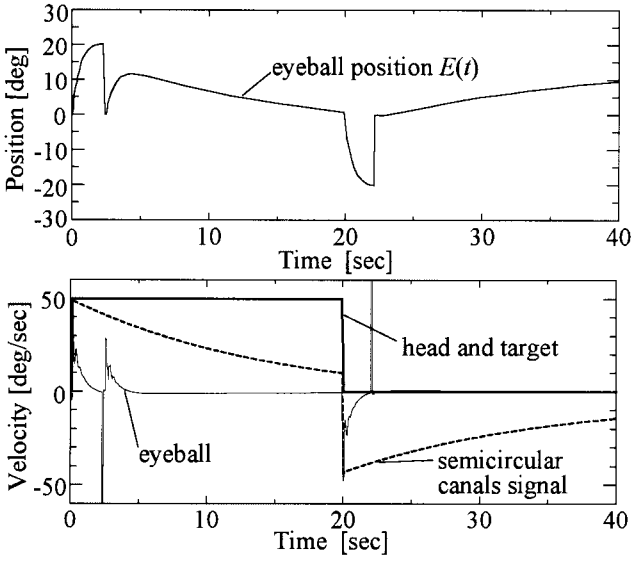

Figure 10. Characteristics of the model when target and head rotate at the same angular velocity.

the following equation is obtained from Equation (2):

$$E(s) = \frac{\alpha T_n T_v s^2}{(T_v s + 1)\{T_n s(1 + \gamma e^{-s\tau}) + 1 + T_n \lambda e^{-s\tau}\}} H(s) \tag{8}$$

The simulation result using Equation (8) is shown in Figure 10. It shows that when head and the target rotate with acceleration, the eye is rotated by the semicircular canals signal (feedforward signal). If head and the target stop or rotate at constant velocity, the signal from semicircular canals become 0, the eyeball is stopped by the retinal slip signal (feedback signal). This phenomenon has also been confirmed by physiological experiments [18].

4. FREQUENCY RESPONSE OF THE MODEL

In the previous section, the performance of the oculomotor model presented was validated by physiological phenomena. The structure of the model is recognized to be consistent with the physiological mechanism.

To understand the relationship between VOR, optokinetic reflex, and smooth pursuit, this section analyses frequency responses of each eye movement type using the oculomotor model. As in the previous section, the same model of Figure 4 is used with $\alpha = 1$, $\gamma = 0.5$, $\lambda = 0.01$. To simplify the discussion, the retinal slip detection delay and the saccadic signal are not taken into consideration.

4.1. Frequency response of VOR

If only VOR is considered, the following frequency transfer function is obtained from Equation (5):

$$\frac{E(\mathrm{j}\omega)}{H(\mathrm{j}\omega)} = \frac{\alpha\omega^2}{(1/T_\mathrm{v}^2 + \omega^2)(1/T_\mathrm{n}^2 + \omega^2)}\left[\left(\omega^2 - \frac{1}{T_\mathrm{v}T_\mathrm{n}}\right) + \left(\frac{1}{T_\mathrm{v}} + \frac{1}{T_\mathrm{n}}\right)\mathrm{j}\omega\right] \tag{9}$$

Figure 11 illustrates the frequency response of Equation (9). It shows that VOR has small response in low frequency domain and shows ideal response in high frequency domain. Gain equal to 1 and phase shift equal to 0° mean that the eyeball rotates at the same velocity as the head in opposite direction.

4.2. Frequency response of optokinetic reflex

If only the optokinetic reflex is considered, $H(s)$ and λ are equal to 0 and the following equation is obtained from Equation (2):

$$\frac{E(s)}{O_\mathrm{t}(s)} = \frac{T_\mathrm{n}\gamma s}{T_\mathrm{n}(1+\gamma)s + 1} \tag{10}$$

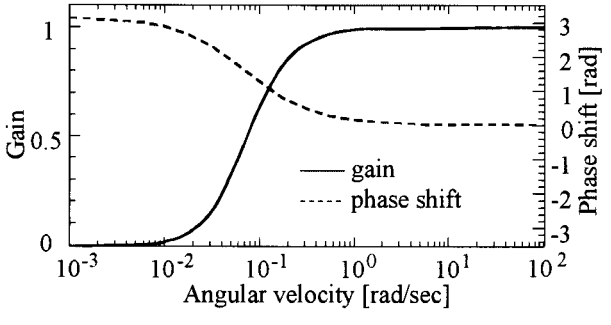

Figure 11. Frequency response of VOR model [11].

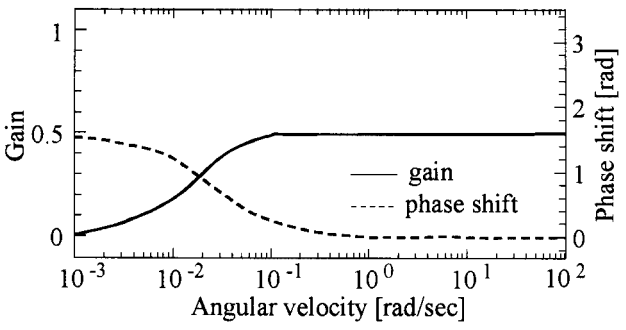

Figure 12. Frequency response of the optokinetic reflex model ($\gamma = 1$, $\alpha = 0$, $\lambda = 0$).

The frequency transfer function is

$$\frac{E(\mathrm{j}\omega)}{O_{\mathrm{t}}(\mathrm{j}\omega)} = \frac{\gamma\omega}{(1+\gamma)^2\omega^2 + 1/T_{\mathrm{n}}^2}\left[(1+\gamma)\omega + \frac{1}{T_{\mathrm{n}}}\mathrm{j}\right] \tag{11}$$

The frequency response is obtained from Equation (11). Figure 12 shows that if gain γ is large enough, the frequency response of optokinetic reflex will become similar to VORs. This phenomenon is demonstrated by physiological experiment, i.e. if the vestibulum is destroyed, the optokinetic reflex will compensate the VOR [3], since the learning system makes γ bigger in this case.

4.3. Frequency response of smooth pursuit

The frequency response of smooth pursuit is obtained when the head is fixed, and gains α and γ in the model are set at zero. In this case the frequency transfer function is

$$\frac{E(\mathrm{j}\omega)}{O_{\mathrm{t}}(\mathrm{j}\omega)} = \frac{\lambda}{(\lambda + 1/T_{\mathrm{n}})^2 + \omega^2}(\lambda + 1/T_{\mathrm{n}} - \mathrm{j}\omega) \tag{12}$$

The frequency response is obtained from Equation (12). Figure 13 shows that the frequency response of smooth pursuit is just the opposite of VORs, i.e. the smooth pursuit only shows good control performance in low-frequency domain.

In fact, physiological smooth pursuit includes control loop of optokinetic reflex and VOR, however, it appears only in low-frequency domain. It becomes clear to interpret smooth pursuit as the retinal slip feedback control from the viewpoint of system control engineering, thus, from now on, the retinal slip feedback control is called smooth pursuit control, and the retinal slip velocity feedback control, as optokinetic reflex control.

4.4 Frequency response of entire eye movement model

As described above, reflex control loop (VOR and optokinetic reflex) shows good performance in high-frequency domain, and smooth pursuit control loop shows good performance in low frequency domain. Thus, the model of eye movement as a whole can be thought as having a 'perfect' performance in all frequency domains.

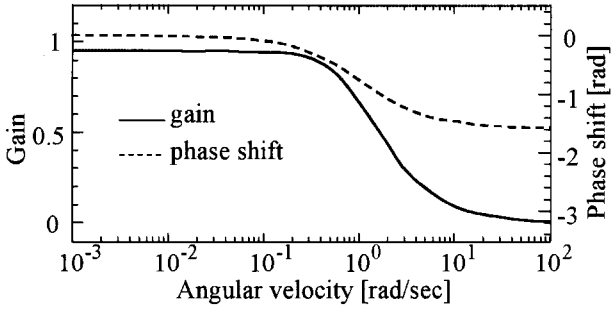

Figure 13. Frequency response of smooth pursuit ($\lambda = 1$).

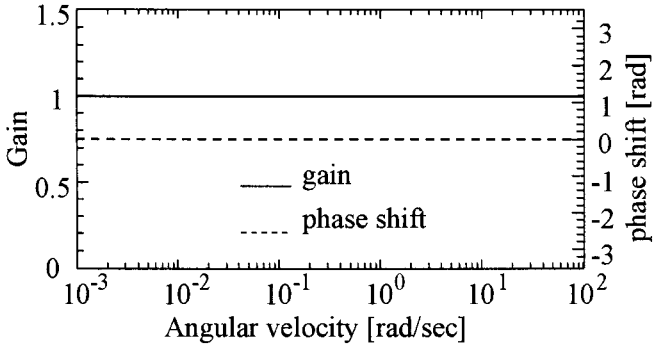

Figure 14. Frequency response of the whole model ($\alpha = \gamma = \lambda = 1$).

Let be discussed below the frequency response of the entire eye movement control model. To ease discussion, the target (drum) is fixed and the head (stand) is rotated. The following equation is derived from Equation (4):

$$\frac{E(s)}{H(s)} = \frac{(\alpha + \gamma) T_v T_n s^2 + T_n(\lambda T_v + \gamma)s + \lambda T_n}{(T_v s + 1)[(1 + \gamma) T_n s + \lambda T_n + 1]} \tag{13}$$

Hence, the frequency transfer function is

$$\frac{E(\mathrm{j}\omega)}{H(\mathrm{j}\omega)} = \frac{-(\alpha + \gamma) T_v T_n \omega^2 + [\lambda T_v + \gamma] T_n \mathrm{j}\omega + \lambda T_n}{(T_v \mathrm{j}\omega + 1)[(1 + \gamma) T_n \mathrm{j}\omega + \lambda T_n + 1]} \tag{14}$$

The frequency response obtained from Equation (14) is shown in Figure 14. It shows a 'perfect' control performance in all frequency domains. However, when the target moves, the control performance gets bad, since the optokinetic reflex control does not possess such a high efficiency in high-frequency domain as VOR.

5. LEARNING SYSTEM OF EYE MOVEMENT MODEL

5.1. *Artificial neural network model*

Flocculi of mammals mainly consist of Purkinje's cells (P), basket cells (B), stellate cells (St), Golgi's cells (G), and granule cells (Gr). The fundamental structure is the same in all flocculi [16]. It can be simplified as shown in Figure 15.

Climbing fibres (cf) and mossy fibres (mf) transfer their input signals to the flocculus. Purkinje's cells' axons transfer the output signals produced by the flocculus to the VN or other nuclei. Each Purkinje's cell is connected to one climbing fibre, and signals from the climbing fibres are considered as processing errors, which are used to improve the synaptic transmission gains of the neural network [16]. Mossy fibres connect to granule cells, and granule cells' axons climb up to the cerebellar cortex and branch into a T shape, becoming parallel fibres. The parallel fibres connect to Purkinje's cells, basket cells, stellate cells, and Golgi's cells to send excitatory signals. Basket cells and stellate cells connect to Purkinje's cells and inhibit them. Golgi's cells connect to granule cells and inhibit them. Figure 16 gives an artificial neural network (ANN) model based on

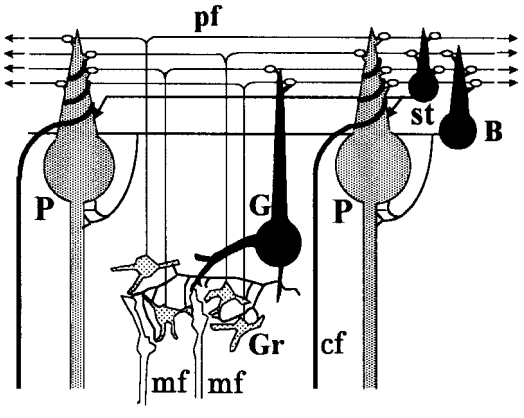

Figure 15. BNN of flocculus [16].

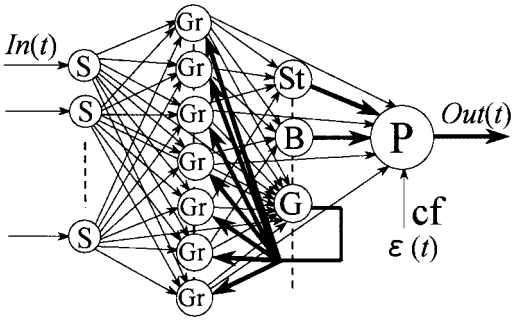

Figure 16. Neural network model of flocculus.

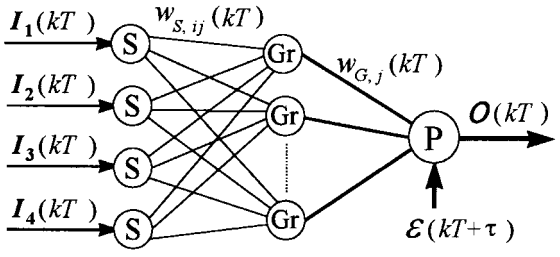

Figure 17. Simplified neural network model of Figure 16.

Figure 15, where S represents origin cells of mossy fibres, and the broken line on nodes St, B, and G means that there are innumerous stellate cells, basket cells, and Golgi's cells.

Golgi's cells are thought as a device to regulate phase difference between signals coming from mossy fibres and from climbing fibres [19]. The role of Golgi's cells can be considered as a compensation for the detection delay of retinal slip $\varepsilon(t)$. Thus, if the Golgi's cells are assumed to be eliminated with their function in the ANN retained, the retinal slip signal appears as $\varepsilon(t+\tau)$ with a detection delay τ. As stellate and basket cells have similar performance, they can be adopted as negative gains from Gr cells to P cell. Thus, if the gain of path number j between Gr cell and P cell is defined as w_{Gj}, and $-\infty < w_{Gj} < \infty$, Figure 17 is obtained from Figure 16. Since the ANN in Figure 2 is a four-input one-output system, Figure 17 was defined as a four-input one-output system, where $\varepsilon(kT+\tau)$ represents retinal slip signal considering the detection delay τ, learning times k and learning cycle time T. As the controlled error at kT is detected at $kT+\tau$, in order to change $w_{S,ij}$ and $w_{G,j}$ within learning period T, $T > \tau$ is required.

Figure 17 shows that the basic structure of flocculus is a two-layered neural network. So, a two-layer ANN using back-propagation algorithm will be adopted in the adaptive eye movement simulations to discuss the relationship between the flocculus learning and VN learning. The conventional ANN learning model with back-propagation method is based on learning by using its output signal error. With respect to biological neural network (BNN) of flocculi, the processing error of controlled object (retinal slip signal) is used in learning.

5.2. The role of ocular muscle's stretch receptors

The stretch receptors of ocular muscles have been thought not to contribute to eye movement. However, neural paths from ocular muscles to flocculus have been known [15]. Here, the role of stretch receptors is discussed in eye movement learning system from the viewpoint of control engineering.

To control an object accurately, a learning control system needs to structure a type of inverse system of the controlled object through learning. In order to characterize a controlled object, its input and output need to be known. That is, the output values of the controlled object are required for the synthesis of its inverse system in the case of learning system, as well as flocculus learning system of eye movement. In Figure 2, the output of the controlled object (ocular muscles and eyeball) is the angle of the optic axis. It is thought that the angle of the optic axis is detected by stretch receptors of the ocular muscles, because the optic axis angle can not be detected by the retina.

5.3. *Learning of vestibular nucleus*

It is known that adaptive performance is not only governed by flocculus, but also by vestibular nucleus [5–9]. Since neurons in vestibular nucleus do not have a complex network structure as flocculus, VN can be considered as a simple learning system that does not have enough ability to make an accurate learning like flocculus, but can learn quickly for its simple structure. This fact is shown by physiological experiments [9].

It is known that ANN learning systems using back-propagation has a contradiction that if the learning constant is small, the convergence speed slows down and easily falls to a local minimum, however if it is set big, the final learning precision becomes bad. The eye movement control system suggests that the whole learning performance is improved by the combination of an ANN with slow and precise learning by setting learning constant small, and a simple learning system with quick convergence. It can be thought that a simple learning system not only improves the total learning speed, but also makes the main learning system avoid local minimums. Thus, the following algorithm is used to simulate learning performance of vestibular nuclei.

$$\alpha(kT + T) = \alpha(kT) + \delta(\rho - \alpha(kT)) + \xi\varepsilon(kT + \tau)H_v(kT + \tau) \tag{15}$$

where, δ is forgetting constant, ρ is standard value of $\alpha(t)$, ξ is learning constant, k is learning times, and T is cycle time. Similar to the previous ANN, $T > \tau$ should be satisfied.

6. SIMULATION OF LEARNING MODEL

Here let the ANN's learning constant be equal to 0.001, number of units of the middle layer be equal to 5, VN learning system's forgetting constant $\delta = 0.001$, standard gain $\rho = 2.5$, learning coefficient $\xi = 0.001$ and $\alpha(0) = 2.5$. Similar to Section 3.1, time constants of the model in Figure 2 are set as $T_v = 15$ s. $T_n = 16$ s, $\tau = 0.12$ s, and $T_e = g_e = 0.01$ s, and visual feedback gains as $\gamma = 0.5$ and $\lambda = 0.01$. The model in Figure 2 is discretized with respect to a sampling time $T_S = 0.005$ s. In fact the learning cycle time of the ANN T would have to be longer than τ. However, if we define $T > \tau$, it will spend too long a time for learning in simulation. Unlike in an organism, the retina slip ε can be calculated within the sampling time T_S in computer simulation, so T is defined equal to T_S. Figure 18 shows the desired value of the eye movement model of Figure 2 that is given by positions of the head and the target. The target rotates

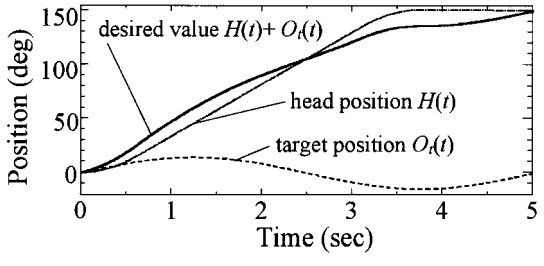

Figure 18. Desired value given by the sum of positions of head and target.

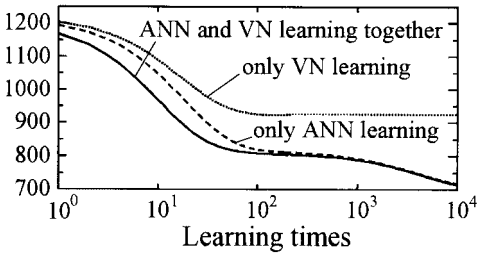

Figure 19. Learning errors $\sum_{k=1}^{n} \varepsilon^2 (kT)$ for eye movement control system learning models.

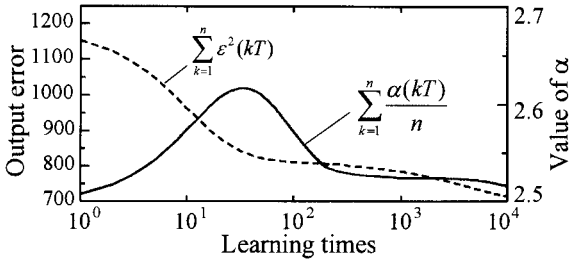

Figure 20. Learning errors $\sum_{k=1}^{n} \varepsilon^2 (kT)$ for eye movement control system learning models.

at $15\sin(2\pi t/5)$ deg/s. The head rotates at an acceleration of 80 deg/s^2 between $t = 0$–0.625 s, at a constant velocity between $t = 0.625$–3.125 s, at an acceleration of -80 deg/s^2 between $t = 3.125$ and 3.750 s and stops to rotate between $t = 3.750$–5 s.

Simulation 1: For discussion of the relationship between the two learning systems, three cases of learning are simulated when the controlled object is set as $g = 0.6$ and $T_e = 0.025$ s. In the simulation, the parameter $\alpha(0)$ is set as 2.5, and the initial weights of the ANN are set according to the learning in normal state ($g = 1$ and $T_e = 0.01$ s). The first case uses only the ANN system for learning. The second case considers only the VN learning system, and the third case uses the two learning systems together. Figure 19 shows sum of squares of the learning errors. It shows, when the ANN system and the VN system work together, both convergence speed and preciseness of learning are better than only the ANN system working by itself. This simulation confirmed that although the VN learning system alone has no high learning ability, it helps the ANN system to make the total learning performance better.

Figure 20 shows, in the beginning of the learning, that $\alpha(t)$ has a rapid increase and it gets back to standard value slowly. This implies that VN plays a main role in the beginning of learning and that ANN plays the leading role in the later period. These phenomena are called, short-and long-term learning in eye movement physiology [9].

Simulation 2: To demonstrate the necessity of the optic axis angle signal in learning, learning performances of the eye movement model are compared before and after cutting the ocular

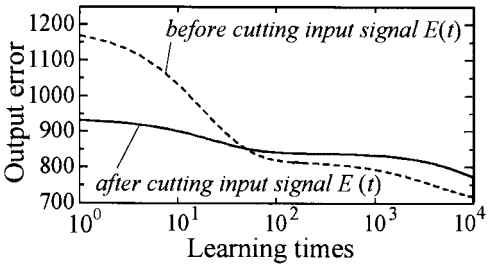

Figure 21. ANN learning errors $\sum_{k=1}^{n} \varepsilon^2 (kT)$ before and after cutting of the stretch receptor signal E.

muscles stretch receptors loop. In the case of a controlled object set by $g = 0.6$, $T_e = 0.025$ s,[§] simulation result of the learning process is shown by Figure 21. The broken line shows learning errors before cutting the feedback loop of the ANN input signal $E(t)$, and the solid line shows learning errors after cutting the loop. It shows that the learning performance after cutting the ANN input signal $E(t)$ is far worse than before cutting.[¶]

7. CONCLUSION

In order to understand how eye movements relate to each other and to analyse the performance of the adaptive mechanism of oculomotor control systems, a unified oculomotor control system model based on eye's anatomical structure and physiological mechanism was proposed. The model was validated by comparing its dynamic characteristics with physiological experiments.

Through the analysis of frequency response of eye movements, the relationship between each eye movement type became clear. That is, in low-frequency domain, eye movement depends on smooth pursuit control loop (the retinal slip signal feedback loop), and in high frequency domain, it depends on VOR (semi-circular canals' signal feedforward loop) and optokinetic reflex control loop (retinal slip velocity signal feedback loop).

Through simulation of adaptive performance of eye movement, the necessity for the two learning systems (the flocculus learning system and the vestibular nucleus learning system) were shown in eye movement control for a single eye. That is, the performance of the two learning systems working together was better than each learning system working by itself.

The role of ocular muscle stretch receptors, i.e. the necessity of optic axis angle signal in flocculus learning when the target is in movement, was confirmed by both system control theory and simulation.

[§]If $g_e = T_e \ll T_n$ is satisfied, Equation (1) is stand, where the denominator $(sT_e + 1)$ of the controlled object can be cancelled by the numerator $(sg_e + 1)$. Thus, the eye movement becomes easy to control. Here $(sg_e + 1)$ is interpreted as a type of inverse system. The inverse system cannot be consistent so long as $T_e = 0.025 \neq g_e$ remains, and the learning system will have to produce an inverse system by learning.

[¶]The beginning of the simulations illustrated by Figure 21, in which the learning errors before cutting the $E(t)$ are bigger than after cutting, provides us the existence of bad influence of signal $E(t)$ on the control system before its adaptation.

ACKNOWLEDGEMENTS

This research was partly supported by Grant-in-Aid for Encouragement of Young Scientists of the Ministry of Education of Japan and the Mitsubishi Foundation.

REFERENCES

1. Cannon SC, Robinson DA. Loss of the neural integrator of the oculomotor system from brain stem lesions in monkey. *Journal of Neurophysiology* 1987; **57**(5):1383–1409.
2. Ito M, Miyashita Y. The effects of chronic destruction of the inferior olive upon visual modification of the horizontal vestibulo-ocular reflex of rabbits. *Proceedings of the Japanese Academy* 1975; **51**:716–720.
3. Ito M. *The Cerebellum and Neural Control*. Raven Press: New York, 1984.
4. Ito M, Sakurai M, Tongroach P. Climbing fiber induced depression of both mossy fiber respond siveness and glutamate sensitivity of cerebellar Purkinje cells. *Journal of Physiology* 1982; **324**:113–134.
5. Lisberger SG. The neural basis for motor learning in the vestibular-ocular reflex in monkeys. *Trends Neurosci* 1988; **11**:147–152.
6. Lisberger SG. The neural basis for learning of simple motor skills. *Science* 1988; **242**:728–735.
7. Lisberger SG, Pavelko T. Brain stem neurons in modified pathways for motor learning in the primate vestibulo-ocular reflex. *Science* 1988; **242**:771–773.
8. Lac S du, Lisberger SG. Eye movements and brain stem neuronal responses evoked by cerebellar and vestibular stimulation in chicks. *Journal of Comparative Physiology A* 1992; **171**(5):629–638.
9. Khater TT, Quinn KJ, Pena J, Baker JF, Peterson BW. The latency of the cat vestibulo-ocular reflex before and after short- and long-term adaptation. *Experimental Brain Research* 1993; **94(1)**:16–32.
10. Wakamatsu H, Kuwano M, Suda H. Hardware control system of eye movement by automatic selection of control laws using neural networks. *Transactions of the IEE Japan* 1994; **114-C**:1024–1030.
11. Wakamatsu H, Zhang X. Optical axis control system as unification of reflex and pursuit eye movements. *Transactions of the IEE Japan* 1997; **117-C(11)**:101–108.
12. Zhang X, Wakamatsu H. Learning model of eye movement system based on anatomical structure. *Transactions of the IEE Japan* 1998; **118-C(7/8)**:1053–1058.
13. Kawato M, Gomi H. The cerebellum and VOR/OKR learning models. *Trends in Neuroscience* 1992; **15(11)**:445–453.
14. Gomi H, Kawato M. Adaptive feedback control models of the vestibulocerebellum and spinocerebellum. *Biological Cybernetics* 1992; **68(2)**:105–114.
15. Maekawa K, Takeda T. Electrophysiological identification of the climbing and mossy fiber pathways from the rabbit's retina to the contralateral cerebellar flocculus. *Brain Research* 1976; **109**:169–174.
16. Ito M, Kano M. Long-lasting depression of parallel fiber-Purkinje cell transmission induced by conjunctive stimulation of parallel fibers and climbing fibers in the cerebellar cortex. *Neuroscience Letters* 1982; **33**:253–258.
17. Cohen B, Matsuo V, Raphan T. Quantitative analysis of the velocity characteristics of optokinetic nystagmus and optokinetic after-nystagmus. *Journal of Physiology*, London 1977; **270**:321–344.
18. Waespe W, Henn B. Conflicting visual–vestibular stimulation and vestibular nucleus activity in alert monkeys. *Experimental Brain Research* 1978; **33**:203–211.
19. Fujita M. Adaptive filter model of the cerebellum. *Biol. Cybern*., 1982; **45**:195–206.
20. Rumelhart DE, Hinton GE, Williams RJ. Learning internal representations by back-propagation errors. *Nature* 1986; **323**:533–536.

